The Gaia-ESO Survey: Abundance ratios in the inner-disk open clusters Trumpler 20, NGC 4815, NGC 6705

L. Magrini, S. Randich, David Romano, E. Friel, A. Bragaglia, R. Smiljanic, H. Jacobson, A. Vallenari, M. Tosi, L. Spina, et al.

A&A 563, A44 (2014)
DOI: 10.1051/0004-6361/201322977

Astronomy & Astrophysics

The *Gaia*-ESO Survey: Abundance ratios in the inner-disk open clusters Trumpler 20, NGC 4815, NGC 6705⋆

L. Magrini[1], S. Randich[1], D. Romano[2], E. Friel[3], A. Bragaglia[2], R. Smiljanic[4,5], H. Jacobson[6], A. Vallenari[7], M. Tosi[2], L. Spina[1,8], P. Donati[2,9], E. Maiorca[1], T. Cantat-Gaudin[7,10], R. Sordo[7], M. Bergemann[11], F. Damiani[12], G. Tautvaišienė[13], S. Blanco-Cuaresma[14,15], F. Jiménez-Esteban[16], D. Geisler[17], N. Mowlavi[18], C. Munoz[17], I. San Roman[17], C. Soubiran[15], S. Villanova[17], S. Zaggia[7], G. Gilmore[11], M. Asplund[19], S. Feltzing[20], R. Jeffries[21], T. Bensby[20], S. Koposov[11,22], A. J. Korn[20], E. Flaccomio[12], E. Pancino[2,23], A. Recio-Blanco[24], G. Sacco[1], M. T. Costado[25], E. Franciosini[1], P. Jofre[11], P. de Laverny[24], V. Hill[24], U. Heiter[26], A. Hourihane[11], R. Jackson[21], C. Lardo[2], L. Morbidelli[1], J. Lewis[11], K. Lind[11], T. Masseron[11], L. Prisinzano[12], and C. Worley[11]

(Affiliations can be found after the references)

Received 4 November 2013 / Accepted 20 December 2013

ABSTRACT

Context. Open clusters are key tools to study the spatial distribution of abundances in the disk and their evolution with time.
Aims. Using the first release of stellar parameters and abundances of the *Gaia*-ESO Survey, we analyse the chemical properties of stars in three old/intermediate-age open clusters, namely NGC 6705, NGC 4815, and Trumpler 20, which are all located in the inner part of the Galactic disk at Galactocentric radius $R_{GC} \sim 7$ kpc. We aim to prove their homogeneity and to compare them with the field population.
Methods. We study the abundance ratios of elements belonging to two different nucleosynthetic channels: α-elements and iron-peak elements. For each element, we analyse the internal chemical homogeneity of cluster members, and we compare the cumulative distributions of cluster abundance ratios with those of solar neighbourhood turn-off stars and of inner-disk/bulge giants. We compare the abundance ratios of field and cluster stars with two chemical evolution models that predict different α-enhancement dependences on the Galactocentric distance due to different assumptions on the infall and star-formation rates.
Results. The main results can be summarised as follows: i) cluster members are chemically homogeneous within 3σ in all analysed elements; ii) the three clusters have comparable [El/Fe] patterns within $\sim 1\sigma$, but they differ in their global metal content [El/H] with NGC 4815 having the lowest metallicity; their [El/Fe] ratios show differences and analogies with those of the field population, in both the solar neighbourhood and the bulge/inner disk; iii) comparing the abundance ratios with the results of two chemical evolution models and with field star abundance distributions, we find that the abundance ratios of Mg, Ni, and Ca in NGC 6705 might require an inner birthplace, implying a subsequent variation in its R_{GC} during its lifetime, which is consistent with previous orbit determination.
Conclusions. Using the results of the first internal data release, we show the potential of the *Gaia*-ESO Survey through a homogeneous and detailed analysis of the cluster versus field populations to reveal the chemical structure of our Galaxy using a completely uniform analysis of different populations. We verify that the *Gaia*-ESO Survey data are able to identify the unique chemical properties of each cluster by pinpointing the composition of the interstellar medium at the epoch and place of formation. The full dataset of the *Gaia*-ESO Survey is a superlative tool to constrain the chemical evolution of our Galaxy by disentangling different formation and evolution scenarios.

Key words. Galaxy: abundances – open clusters and associations: general – open clusters and associations: individual: Trumpler 20 – open clusters and associations: individual: NGC 4815 – globular clusters: individual: NGC 6705 – Galaxy: disk

1. Introduction

Open clusters are very useful tracers of the processes of formation and evolution of our Galaxy. They are a disk population located from the inner parts of the disk to its outskirts with ages spanning from a few Myr for recently formed clusters to several Gyr for old clusters (see, e.g., Dias et al. 2002; Dias et al. 2012). The population of young open clusters has a small scale height above the Galactic plane (~60 pc), while old open clusters reach higher altitudes ~350 pc (Chen et al. 2003), thus presumably being all part of the thin component of the disk. Kinematics of open clusters, in both terms of rotation and velocity dispersions are also consistent with the association of the thin disk of the Galaxy (Scott et al. 1995; Wu et al. 2009). In addition, form a chemical point of view, the roughly solar abundance ratios of open clusters further support to an association with the thin disk.

Their ages and distances can be derived from colour−magnitude diagrams, which are obtained via photometric studies. This makes them a perfect instrument to investigate the temporal changes in the spatial distribution of abundances (e.g., Magrini et al. 2009; Yong et al. 2012).

In the framework of the study of cluster population, the *Gaia*-ESO Survey (Gilmore et al. 2012; Randich & Gilmore 2012) with other spectroscopic surveys observing open clusters, such as the Apache Point Observatory Galactic Evolution Experiment (APOGEE, Allende-Prieto et al. 2008), is allowing us to study a large number of young, intermediate-age, and old open clusters. Within the APOGEE project, the Open Cluster Chemical Analysis and Mapping (OCCAM) survey aims to produce a comprehensive, uniform infrared-based data set for hundreds of open clusters and to constrain key Galactic

⋆ Based on observations collected with the FLAMES spectrograph at the VLT/UT2 telescope (Paranal Observatory, ESO, Chile), for the *Gaia*-ESO Large Public Survey (188.B-3002).

dynamical and chemical parameters from this sample. A first contribution to the OCCAM project has been recently published by Frinchaboy et al. (2013) that presented the analysis of 141 members stars in 28 open clusters. This new dataset allowed them to revise the Galactic metallicity gradient.

In particular, old and intermediate-age clusters are rare fossils of the past star-formation history of the Galactic disk. Apparently, the old open clusters observed at present time with ages over ~1 Gyr have survived because of their peculiar initial characteristics, such as their larger than average mass, higher central concentration, and orbits that allow them to avoid the disruptive influence of the giant molecular clouds (Friel 1995; Janes & Phelps 1994; Bonatto et al. 2006). This might introduce possible differences in chemical composition between field and cluster stars presently observed at the same Galactocentric radius, since both might have moved from their place of birth but in different ways.

The majority of stars born in open clusters were indeed dispersed into the Galaxy field in a relatively short time within the first Gyr from their formation (see, e.g., Janes & Phelps 1994; Lada & Lada 2003; Gieles et al. 2006). This phenomenon is more rapid in the inner disk, where the density of stars is higher (Freeman 1970; van der Kruit 2002). Thus, the existence of several old and intermediate-age open clusters within the Solar circle ($R_{GC} < 8$ kpc), such as those observed during the first periods of observation of the *Gaia*-ESO Survey, offers a unique opportunity to study the evolution of the disk in a region so far little explored.

Specifically, this study focuses on detailed and homogeneously obtained chemical abundance patterns of different populations that offer valuable clues in the interpretation of the Galactic history. We refer to the paper of Jacobson et al. (in prep.) for a discussion of the spatial distribution of the global metallicity and its implications for the radial Galactic metallicity gradient.

As a first approximation, we expect the abundances of open clusters to match those of the field stars at similar Galactocentric distances, but observations are revealing differences (see, e.g., Yong et al. 2005, 2012; De Silva et al. 2007) and these differences contain important information, such as the place where the open clusters were born, the homogeneity of the disk at any R_{GC} at the epoch when the cluster formed, etc.

In more detail, studies that compare field and cluster populations were tackled by several authors in the past. For example, De Silva et al. (2007) analysed the chemical pattern of the inner old open cluster Collinder 261 by comparing its abundance ratios with those of Cepheid stars and of field stars. They found remarkable differences for some elements, such as Na, Mg, Si, and Ba. They claimed that the differences are a signature of the local inhomogeneities at the time and site of cluster formation. Other examples can be found in the works of Yong et al. (2005, 2012) and of Sestito et al. (2008), who studied open clusters located at $R_{GC} > 13$ kpc. They compared the chemical properties of several outer disk open clusters to those of stellar clusters located in the disk within $R_{GC} < 13$ kpc and to other stellar tracers that are located in the outer disk, such as red giant stars, Cepheids, and the solar neighbourhood stars. They found that the behaviour of α-elements is not exactly the same in all their clusters but that it is on average similar to that of solar neighbourhood stars. They concluded that the primary difference between the solar neighbourhood and outer disk is that the chemical enrichment in the outer disk did not yet reach the metallicities of the solar neighbourhood, but the contribution of the two nucleosynthetic channels, SNII and SNIa, appear to have been similar. However, the conclusions of these works are usually based on heterogeneous samples, including literature and the authors' own results. Heterogeneous samples might mask genuine abundance differences and/or artificially induce (or amplify) abundance differences between otherwise chemically similar populations. The different effects are driven by the size of the samples and by the elements considered.

In this framework the *Gaia*-ESO Survey data with its uniform dataset and its homogeneous analysis, will allows for the first time a comparison of different populations on a footing not possible before.

As an initial step in this direction, the first data release of the *Gaia*-ESO Survey, including the first six months of observations, allows us to analyse the chemical composition of three old and intermediate-age open clusters located in the very inner disk (NGC 6705, NGC 4815, and Trumpler 20), and to compare them with the field population in the solar neighbourhood and with evolved stars located in the inner-disk/bulge in detail.

The present paper is structured as follows: in Sect. 2, we briefly describe the *Gaia*-ESO Survey. In Sect. 3, we present the properties and membership of the first three old/intermediate-age clusters observed by the *Gaia*-ESO Survey. In Sect. 4, we summarise the target selection strategy for field stars. In Sect. 5, we check the quality of the analysis of cluster stars and we analyse the abundance patterns of the three open cluster and compare them to the field population, whereas we speculate on the origin of their abundance ratios in Sect. 6. In Sect. 7, we give our summary.

2. The *Gaia*-ESO Survey and its first data release

The *Gaia*-ESO Survey is a large, public spectroscopic survey that started at the end of 2011 that is employing the VLT FLAMES (Pasquini et al. 2002) instrument to obtain high quality spectroscopy of $\sim 10^5$ stars in our Galaxy. The observed stars belong to well defined samples and are selected by making use of several photometric databases, such as the VISTA Hemisphere Survey (VHS; McMahon 2012), the Two Micron All Sky Survey (2MASS, Skrutskie et al. 2006), and a variety of photometric surveys of open clusters. The focus of the *Gaia*-ESO Survey is to quantify the kinematical and chemical element abundance distributions in the different components of the Milky Way: bulge, thin and thick disks, halo, and about a hundred open clusters that span a large range of ages, distances, and masses. A general description of the Survey can be found in Gilmore et al. (in prep.) and Randich et al. (in prep.).

In the present work, we discuss results from the analysis of UVES (Dekker et al. 2000) spectra of F-G-K stars. This analysis is described in detail in Smiljanic et al. (in prep.). We briefly review how recommended parameters are computed. The recommended parameters are obtained by combining the results of different nodes which consider first the accuracy of each node judged using a sample of calibration stars with well-known stellar parameters, called benchmark stars, as a reference (see Jofre et al. 2013a,b). Among the benchmark stars, there are stars having stellar parameters comparable to that of the stars discussed in the present paper, as ξ Hya.

The different approaches of the nodes can be summarised as follows: *i)* nodes that employ the equivalent width (EW) analysis, obtaining EWs form the observed spectra; the atmospheric parameter determination is based on the excitation and ionisation balance of iron lines; *ii)* spectrum synthesis methods derive the atmospheric parameters from a χ^2 fit to observed spectra; in

Table 1. Clusters' parameters.

Name	α J2000.0	δ J2000.0	l (deg)	b (deg)	$E(B-V)$	Age (Gyr)	TO mass ($M_\odot$)	$D_\odot$ (kpc)	R_{GC}[d] (kpc)	[Fe/H]	N. of members
NGC 6705[a]	18:51:05	–06:16:12	27.31	–2.78	0.43	0.30 ± 0.05	∼3	1.9	6.3	+0.14 ± 0.06	21
Trumpler20[b]	12:39:32	–60:37:36	301.48	2.22	0.33	1.50 ± 0.15	∼1.8	2.4	6.88	+0.17 ± 0.05	13
NGC 4815[c]	12:57:59	–64:57:36	303.63	–2.10	0.72	0.57 ± 0.07	∼2.5	2.5	6.9	+0.03 ± 0.05	5

Notes. [(a)] NGC 6705 parameters from Cantat-Gaudin et al. (in prep.); [(b)] Trumpler 20 parameters from Donati et al. (2014); [(c)] NGC 4815 parameters from Friel et al. (in prep.); [(d)] computed with $R_\odot$ = 8 kpc.

some cases, the computation of EWs from best-matching synthetic spectra is used to derive the individual element abundances; *iii)* multi-linear regression methods that simultaneously determine the stellar parameters of an observed spectrum by the projection of the spectrum onto vector functions, constructed as an optimal linear combination of the local synthetic spectra.

Eights nodes use the EW method, while the remaining five nodes adopt different approaches to the spectral synthesis. Details on the individual node techniques are in Smiljanic et al. (in prep.).

Further consistency tests are conducted using the calibration clusters, and other calibration targets, such as the globular clusters and the CoRoT giant stars (COnvection ROtation and planetary Transits, Baglin et al. 2006). The nodes' and recommended parameters of NGC 1851 and NGC 2808 were compared to PARSEC isochrones in the $T_{\rm eff}$ vs. log g plane and found to agree. Then the parts of the parameter space where a given node under-performs are identified[1].

Finally, the median value of the validated results is adopted as the recommended value of that parameter. For the cluster stars discussed in the present paper, the recommended values are typically derived using the results of 8−10 nodes. For the solar neighbourhood stars and the inner-disk/bulge stars, the parameters are, on average, determined using the results of nine nodes.

The uncertainties are taken to be the method-to-method dispersions. Once the recommended values of the atmospheric parameters of all stars are defined, the spectroscopic analysis proceeds to its second step, the determination of elemental abundances. The nodes use the recommended parameters to recompute elemental abundances, and the median values of the resulting abundances are the final recommended best values.

We emphasise here that cluster and field stars are analysed in a completely homogeneous way. Parameters and abundances for stars observed during the first six months have been delivered within the *Gaia*-ESO Survey consortium in an internal Data Release (GESviDR1Final), which includes abundances of FeI, FeII, NiI, CrI, TiI, TiII, SiI, CaI, MgI, NaI, AlI, ZnI, YII, ZrII, and CeII. Unfortunately, the abundances of neutron capture elements are available only for a small sub-sample of stars, and thus, they are not discussed in the present paper. The recommended values are used in the rest of the paper. In particular, we use the abundances derived with the recommended parameters, including those of iron (computed considering only Fe I lines). The *Gaia*-ESO survey abundances are scaled to the solar abundances of Grevesse et al. (2007). The errors on [Fe/H] are comparable among the different samples of solar-neighbourhood stars, inner disk stars, and intermediate-age cluster stars as discussed in the present paper with cool stars that have higher errors in both cluster and Milky Way stars in general. Typical errors are of the order of 0.1 dex, and they become ∼0.2 dex for several stars cooler than ∼4500 K.

[1] Nodes that cannot analyse the benchmark stars and reproduce their atmospheric parameters ($T_{\rm eff}$ and log g) within 150 K and 0.30 dex, respectively, are disregarded.

3. The old and intermediate-age clusters in DR1

Three old and intermediate-age open clusters were observed and analysed in DR 1: NGC 6705, NGC 4815, and Trumpler 20. They are all located within the Solar circle in a region that is still poorly investigated but of great importance for our understanding of the mechanisms of disk/bulge formation. Being close to the Galactic centre (see Table 1), the three clusters might suffer from strong tidal effects and frequent interactions with molecular clouds, and thus they can provide important constraints to the cluster survival in a "hostile" environment (see, e.g., Janes & Phelps 1994; Lada & Lada 2003; Gieles et al. 2006). They might also probe a key issue to understand the mechanism of Galaxy formation and evolution, or the radial metallicity gradient, which has been the subject of a number of studies in past decades using open clusters as tracers (see, e.g., Janes 1979; Panagia & Tosi 1981; Friel 1995; Twarog et al. 1997; Carraro et al. 1998; Bragaglia & Tosi 2006; Sestito et al. 2006, 2007, 2008; Magrini et al. 2009; Pancino et al. 2010; Andreuzzi et al. 2011; Jacobson et al. 2011). The first results from the *Gaia*-ESO Survey are helping to shed light on the radial metallicity gradient in the very inner part of the disk, (Jacobson et al., in prep.). Stars observed in the three clusters were selected on the basis of their colour−magnitude diagrams: targets for GIRAFFE were mainly main-sequence stars, while targets for UVES were evolved stars belonging to the red clump. More details on target selection can be found in Bragaglia et al. (in prep.) and the papers on individual clusters, as Donati et al. (2014) for Trumpler 20 and Friel et al. (in prep.) for NGC 4815.

In the present paper, we show the results of [Fe/H] and abundance ratios of member stars of the three clusters presented above and observed with UVES. The membership has been derived using the information on the radial velocities, as measured in the *Gaia*-ESO Survey spectra in the paper of Donati et al. (2014) for Trumpler 20, in Friel et al. (in prep.) for NGC 4815, and in Cantat-Gaudin et al. (in prep.) for NGC 6705. Briefly, the radial velocities are first used to identify the systemic velocity of the cluster and then to remove stars beyond a certain σ level from the median velocity to separate cluster member stars from the field.

The cluster parameters are summarised in Table 1, where we show the names of the clusters, their coordinates (equatorial and Galactic), the reddening $E(B-V)$, the age in Gyr, the turn-off (TO) mass in solar masses, the distance from the Sun, the Galactocentric distance, the height from the Galactic plane in kpc, the metallicity, [Fe/H], and the number of members analysed. For a discussion and comparison to literature values of the three clusters, we refer to the papers of Donati et al. (2014), Friel et al. (in prep.), and Cantat-Gaudin et al. (in prep.).

4. UVES observations of field stars in DR1

To compare the abundance ratios of the different populations of the Milky Way and of open clusters in a fully homogeneous way, we have considered the results in GESviDR1Final for the Milky Way field stars. These stars belong to two samples: the solar neighbourhood sample and the bulge/inner disk sample. For a complete description about how these samples are defined, we refer to Gilmore et al. (in prep.).

The solar neighbourhood sample. The observation criteria for the UVES stars aim to include the three major solar neighbourhood population groups (halo, thick disk, and old thin disk). They are designed to obtain an unbiased sample of ~5000 G-stars within 2 kpc from the Sun. The purpose of this sample is to quantify the local elemental abundance distribution functions in detail. The sample used for the present work includes 390 stars and corresponds to the Milky Way turn-off (TO) stars with recommended parameters in GESviDR1Final.

The bulge and inner disk. The UVES stars observed with the GIRAFFE stars that are dedicated to the study of Galactic bulge are expected to be evolved stars belonging to both bulge and inner disk populations. The prime targets of the GIRAFFE observations are K giants, including the red clump stars, with typical magnitude $I = 15$. The brighter K giant stars in the same fields are the targets of UVES, and they allow sampling bulge and inner Galaxy populations. During the first six months of the *Gaia*-ESO Survey, 32 stars of the bulge/inner-disk were observed and are included in the present discussion.

5. The abundance patterns of open clusters

The first step of our analysis is thus to check if the abundance ratios in each clusters are independent of the stellar parameters. To derive the abundance ratios we use the iron abundance computed by the nodes with the recommended stellar parameters. In Table 2 we present the ids, the radial velocities, the recommended values of stellar parameters ($T_{\rm eff}$, log g and ξ) with their errors and the elemental abundance with their error (expressed in the logarithmic form $A(\mathrm{El}) = 12 + \log(\mathrm{El/H})$) for members in open clusters. As anticipated in Sect. 2, the uncertainties on the stellar parameters ($T_{\rm eff}$, log g, ξ and [Fe/H]) in DR 1 are the method-to-method dispersions. For Fe I, two errors are given: the method-to-method dispersion (σ (FeI), in Col. 6) computed in the calculation of the recommended atmospheric parameters and the node-to-node dispersion in A(FeI) of abundances re-computed with the recommended parameters (the error on [Fe/H] presented in Col. 5).

The results are shown in Fig. 1 for [Fe/H] and in Fig. 2 for [El/Fe]. In Fig. 1 we plot the stellar parameters versus [Fe/H] for member stars in the three clusters. We also show the mean least squares fits to the data for NGC 6705 and NGC 4815. We do not plot the linear fits for Trumpler 20, since they are artificially driven by the small interval that is spanned in stellar parameters by its member stars. The trends are almost absent for NGC 4815, while some trends are present for NGC 6705, even if the ranges in $T_{\rm eff}$, log g and ξ spanned by its members are again small.

In Fig. 2 the plots of [El/Fe] versus stellar parameters are shown. The trends of $T_{\rm eff}$ and log g are almost zero for all elements for NGC 6705 and Trumpler 20 where we have greater statistics, with a possible exception of [Mg/Fe]. The trends of ξ seem to be more important and might affect more elements. In general, the cluster stars do not show important trends which could affect our further analysis.

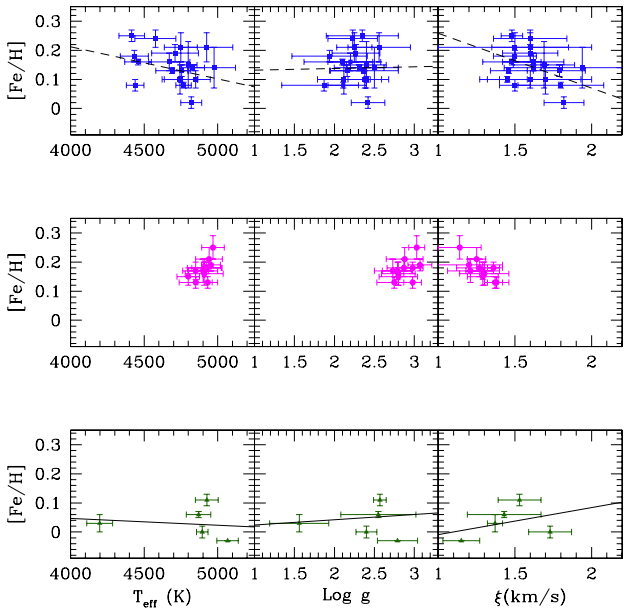

Fig. 1. [Fe/H] versus stellar parameters in the three clusters. The results of NGC 6705 (blue) are shown in the *upper panels*, while Trumpler 20 (magenta) is in the *middle panels* and NGC 4815 (dark green) in the *bottom panels*.

5.1. Confirming the chemical homogeneity of clusters

It is often stated that open clusters are among the best objects for tracing the star-formation history in the disk (see, e.g., Friel 1995). They are considered to be composed of simple stellar populations, which are homogeneous in terms of age and chemical composition. Thus, we investigate the degree of homogeneity of the abundances of cluster members. We compare the standard deviation (σ) of all elements with the average uncertainty in the abundances ($\Delta = \langle\delta\rangle$), which is computed by averaging the error on abundance ratios of each member star (δ). We considered the cluster homogeneous in a specified element if the intrinsic scatter, as given by the σ, is lower or comparable to the average error Δ, which should be indicative of the expected dispersion.

The results are shown in Table 3 and in Figs. 3–5. The rectangles indicate the regions which are 1σ wide around the average. The three clusters are essentially homogeneous in all elements. For Trumpler 20 we notice the presence of a star (#12391577-6034406) that is slightly metal poorer than the main body of cluster members. However, its radial velocity and stellar parameters agree with those of the other observed clump stars. As discussed in Donati et al. (2014), the Besançon model (Robin et al. 2003) computed at the location of Trumpler 20 indicates that 17% of the candidate members for radial velocities may be still field stars. This corresponds to ~1−2 stars being possibly non-members in a sample of 13 stars, and it could justify the lower [Fe/H] of #12391577-6034406. For NGC 6705, we note a possible bi-modal behaviour of [Mg/Fe] with four stars outside the 1σ rectangle around the average (see also the trends in Figs. 2).

In Table 3, we report the following for each cluster: the abundance ratios, the standard deviation σ, the average error on each measurement, Δ, and the number of stars used to compute these quantities. For [El/Fe] ratios, Δ takes into account the errors on [El/H] and [Fe/H], as summed in quadrature. We note, however,

Table 2. Stellar parameters and abundance for member stars.

Id	$T_{\rm eff}$ K	log g	ξ km s^{-1}	A(FeI)	σ (FeI)	A(FeII)	A(MgI)	A(SiI)	A(CaI)	A(TiI)	A(CrI)	A(NiI)
12391577-6034406	4849 ± 41	2.86 ± 0.13	1.27 ± 0.11	7.50 ± 0.03	0.06	7.46 ± 0.05	7.67 ± 0.09	7.54 ± 0.05	6.38 ± 0.05	4.91 ± 0.02	5.66 ± 0.07	6.18 ± 0.03
12392585-6038279	5034 ± 106	3.12 ± 0.31	1.25 ± 0.1	7.66 ± 0.01	0.08	7.64 ± 0.07	7.79 ± 0.06	7.70 ± 0.04	6.46 ± 0.01	5.04 ± 0.02	5.81 ± 0.03	6.37 ± 0.01
12392700-6036053	4800 ± 77	2.80 ± 0.24	1.29 ± 0.1	7.60 ± 0.03	0.07	7.57 ± 0.04	7.72 ± 0.02	7.63 ± 0.06	6.38 ± 0.04	4.91 ± 0.03	5.67 ± 0.02	6.34 ± 0.04
12393132-6039422	4954 ± 64	3.07 ± 0.15	1.20 ± 0.22	7.64 ± 0.02	0.05	7.67 ± 0.06	7.75 ± 0.02	7.68 ± 0.04	6.47 ± 0.05	5.01 ± 0.03	5.76 ± 0.06	6.37 ± 0.02
12393782-6039051	4909 ± 129	2.80 ± 0.21	1.30 ± 0.16	7.61 ± 0.04	0.12	7.62 ± 0.06	7.75 ± 0.06	7.66 ± 0.04	6.42 ± 0.04	4.97 ± 0.01	5.71 ± 0.02	6.32 ± 0.02
12394419-6034412	4941 ± 90	2.88 ± 0.23	1.25 ± 0.06	7.66 ± 0.04	0.07	7.67 ± 0.03	7.75 ± 0.04	7.64 ± 0.05	6.50 ± 0.03	5.03 ± 0.02	5.76 ± 0.03	6.38 ± 0.01
12394475-6038339	4850 ± 112	2.75 ± 0.22	1.38 ± 0.08	7.58 ± 0.02	0.05	7.62 ± 0.06	7.75 ± 0.04	7.66 ± 0.02	6.39 ± 0.02	4.93 ± 0.04	5.71 ± 0.04	6.32 ± 0.02
12394596-6038389	4912 ± 118	2.87 ± 0.21	1.27 ± 0.15	7.63 ± 0.03	0.06	7.64 ± 0.04	7.72 ± 0.05	7.63 ± 0.04	6.44 ± 0.07	4.94 ± 0.02	5.71 ± 0.01	6.34 ± 0.04
12394690-6033540	4968 ± 77	3.03 ± 0.1	1.14 ± 0.14	7.70 ± 0.04	0.11	7.69 ± 0.04	7.79 ± 0.04	7.70 ± 0.05	6.47 ± 0.04	5.01 ± 0.01	5.76 ± 0.03	6.42 ± 0.02
12394742-6038411	4900 ± 100	2.73 ± 0.23	1.21 ± 0.15	7.62 ± 0.04	0.05	7.59 ± 0.02	7.75 ± 0.04	7.70 ± 0.02	6.43 ± 0.04	4.94 ± 0.01	5.73 ± 0.03	6.32 ± 0.03
12395426-6038369	4925 ± 100	2.98 ± 0.13	1.36 ± 0.04	7.63 ± 0.02	0.07	7.66 ± 0.08	7.74 ± 0.05	7.67 ± 0.04	6.42 ± 0.03	5.01 ± 0.02	5.72 ± 0.06	6.37 ± 0.02
12395975-6035072	4850 ± 87	2.79 ± 0.19	1.29 ± 0.11	7.62 ± 0.03	0.07	7.61 ± 0.08	7.74 ± 0.06	7.67 ± 0.03	6.42 ± 0.03	4.92 ± 0.03	5.69 ± 0.03	6.31 ± 0.02
12400278-6041192	4932 ± 67	2.98 ± 0.11	1.37 ± 0.05	7.58 ± 0.02	0.10	7.61 ± 0.07	7.71 ± 0.07	7.66 ± 0.03	6.42 ± 0.03	4.96 ± 0.03	5.71 ± 0.07	6.32 ± 0.04
12572442-6455173	4198 ± 88	1.56 ± 0.37	1.37 ± 0.05	7.48 ± 0.03	0.07	7.53 ± 0.03	7.85 ± 0.04	7.6 ± 0.1	6.23 ± 0.07	4.66 ± 0.03	5.5 ± 0.01	6.2 ± 0.04
12574328-6457386	4895 ± 40	2.40 ± 0.13	1.73 ± 0.14	7.45 ± 0.02	0.08	7.46 ± 0.05	7.68 ± 0.1	7.47 ± 0.05	6.29 ± 0.05	4.75 ± 0.03	5.54 ± 0.03	6.13 ± 0.04
12575511-6458483	4870 ± 84	2.55 ± 0.47	1.43 ± 0.24	7.51 ± 0.01	0.07	7.55 ± 0.06	7.78 ± 0.07	7.5 ± 0.01	6.32 ± 0.02	4.8 ± 0.03	5.56 ± 0.07	6.18 ± 0.08
12575529-6456536	5068 ± 73	2.79 ± 0.25	1.15 ± 0.12	7.42 ± 0.01	0.09	7.42 ± 0.03	7.53 ± 0.16	7.42 ± 0.05	6.22 ± 0.03	4.77 ± 0.02	5.44 ± 0.07	6.11 ± 0.05
12580262-6456492	4926 ± 77	2.57 ± 0.08	1.53 ± 0.14	7.56 ± 0.02	0.06	7.55 ± 0.04	7.69 ± 0.17	7.62 ± 0.04	6.37 ± 0.05	4.91 ± 0.02	5.6 ± 0.05	6.23 ± 0.01
18503724-0614364	4820 ± 71	2.42 ± 0.21	1.82 ± 0.13	7.47 ± 0.02	0.14	7.54 ± 0.08	7.78 ± 0.09	7.62 ± 0.05	6.3 ± 0.07	4.83 ± 0.0	5.62 ± 0.04	6.21 ± 0.07
18504737-0617184	4325 ± 130	1.72 ± 0.29	1.56 ± 0.16	7.54 ± 0.04	0.15	7.54 ± 0.16	7.85 ± 0.03	7.63 ± 0.08	6.35 ± 0.05	4.87 ± 0.05	5.64 ± 0.04	6.3 ± 0.01
18505494-0616182	4689 ± 109	2.37 ± 0.43	1.46 ± 0.12	7.58 ± 0.01	0.09	7.6 ± 0.1	7.8 ± 0.03	7.71 ± 0.03	6.42 ± 0.04	5.01 ± 0.06	5.75 ± 0.09	6.38 ± 0.02
18505581-0618148	4577 ± 139	2.23 ± 0.31	1.60 ± 0.24	7.69 ± 0.03	0.18	7.61 ± 0.08	7.89 ± 0.08	7.8 ± 0.05	6.49 ± 0.02	5.16 ± 0.04	5.8 ± 0.09	6.49 ± 0.01
18505755-0613461	4873 ± 114	2.37 ± 0.32	1.33 ± 0.19	7.53 ± 0.04	0.14	7.38 ± 0.01	7.71 ± 0.04	7.66 ± 0.04	6.46 ± 0.1	4.87 ± 0.07	5.59 ± 0.03	6.21 ± 0.15
18505944-0612435	4925 ± 177	2.56 ± 0.39	1.50 ± 0.5	7.66 ± 0.05	0.18	7.68 ± 0.07	7.88 ± 0.12	7.68 ± 0.06	6.42 ± 0.12	5.01 ± 0.04	5.79 ± 0.07	6.4 ± 0.05
18510023-0616594	4433 ± 95	1.94 ± 0.47	1.50 ± 0.14	7.63 ± 0.02	0.12	7.58 ± 0.13	7.91 ± 0.1	7.71 ± 0.13	6.42 ± 0.02	5.05 ± 0.02	5.75 ± 0.07	6.45 ± 0.01
18510032-0617183	4850 ± 100	2.38 ± 0.21	1.60 ± 0.33	7.55 ± 0.03	0.15	7.55 ± 0.09	7.84 ± 0.1	7.63 ± 0.06	6.43 ± 0.08	4.94 ± 0.03	5.68 ± 0.02	6.31 ± 0.04
18510200-0617265	4415 ± 87	2.35 ± 0.45	1.48 ± 0.07	7.7 ± 0.02	0.14	7.82 ± 0.1	7.94 ± 0.08	7.78 ± 0.06	6.48 ± 0.01	5.03 ± 0.02	5.7 ± 0.02	6.47 ± 0.02
18510289-0615301	4750 ± 112	2.40 ± 0.28	1.45 ± 0.13	7.55 ± 0.01	0.07	7.53 ± 0.08	7.76 ± 0.11	7.66 ± 0.06	6.44 ± 0.06	5.02 ± 0.02	5.73 ± 0.06	6.32 ± 0.04
18510341-0616202	4975 ± 146	2.50 ± 0.3	1.94 ± 0.27	7.59 ± 0.07	0.15	7.46 ± 0.07	7.97 ± 0.06	7.58 ± 0.07	6.42 ± 0.07	5.15 ± 0.02	5.75 ± 0.06	6.31 ± 0.0
18510358-0616112	4832 ± 79	2.31 ± 0.31	1.62 ± 0.19	7.59 ± 0.01	0.08	7.62 ± 0.11	7.79 ± 0.06	7.72 ± 0.08	6.44 ± 0.01	4.98 ± 0.05	5.68 ± 0.02	6.36 ± 0.02
18510786-0617119	4768 ± 53	2.11 ± 0.19	1.80 ± 0.28	7.53 ± 0.01	0.14	7.49 ± 0.04	8.03 ± 0.01	7.67 ± 0.11	6.45 ± 0.02	5.0 ± 0.01	5.72 ± 0.06	6.29 ± 0.03
18510833-0616532	4750 ± 112	2.25 ± 0.22	1.60 ± 0.25	7.66 ± 0.05	0.10	7.62 ± 0.04	7.93 ± 0.1	7.66 ± 0.07	6.45 ± 0.02	4.96 ± 0.02	5.78 ± 0.12	6.44 ± 0.02
18511013-0615486	4439 ± 59	1.87 ± 0.53	1.50 ± 0.1	7.53 ± 0.02	0.12	7.51 ± 0.09	7.84 ± 0.1	7.66 ± 0.08	6.35 ± 0.01	4.82 ± 0.05	5.6 ± 0.03	6.34 ± 0.04
18511048-0615470	4744 ± 122	2.12 ± 0.33	1.70 ± 0.3	7.55 ± 0.05	0.14	7.53 ± 0.11	8.02 ± 0.03	7.58 ± 0.18	6.41 ± 0.06	4.98 ± 0.04	5.71 ± 0.01	6.31 ± 0.01
18511452-0616551	4800 ± 59	2.40 ± 0.25	1.69 ± 0.2	7.6 ± 0.08	0.08	7.63 ± 0.04	7.83 ± 0.28	7.72 ± 0.08	6.48 ± 0.07	5.03 ± 0.04	5.72 ± 0.03	6.39 ± 0.02
18511534-0618359	4755 ± 57	2.16 ± 0.21	1.79 ± 0.17	7.58 ± 0.02	0.22	7.53 ± 0.01	7.99 ± 0.09	7.72 ± 0.1	6.45 ± 0.03	5.03 ± 0.04	5.77 ± 0.04	6.36 ± 0.03
18511571-0618146	4710 ± 159	2.27 ± 0.3	1.60 ± 0.18	7.64 ± 0.03	0.12	7.66 ± 0.04	7.81 ± 0.12	7.7 ± 0.04	6.45 ± 0.04	5.0 ± 0.02	5.74 ± 0.04	6.43 ± 0.02
18512662-0614537	4459 ± 91	2.10 ± 0.48	1.48 ± 0.19	7.61 ± 0.01	0.17	7.61 ± 0.09	7.93 ± 0.14	7.8 ± 0.14	6.45 ± 0.02	5.11 ± 0.06	5.75 ± 0.06	6.44 ± 0.01
18514130-0620125	4671 ± 140	2.20 ± 0.28	1.62 ± 0.2	7.61 ± 0.03	0.19	7.55 ± 0.09	7.8 ± 0.1	7.68 ± 0.06	6.41 ± 0.0	4.93 ± 0.01	5.74 ± 0.04	6.37 ± 0.01

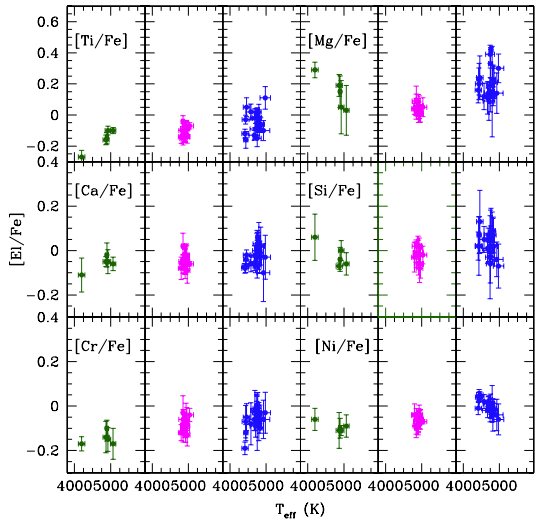

(a) Temperature

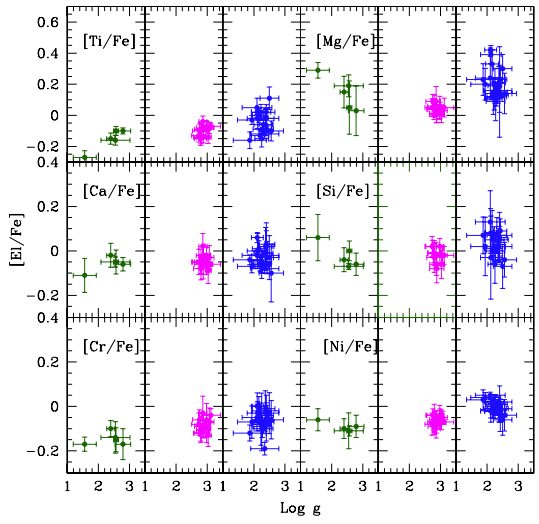

(b) Gravity

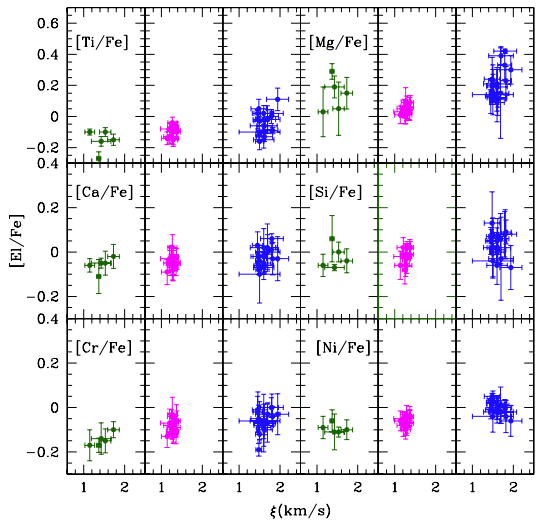

(c) Microturbulence

Fig. 2. Abundance ratios versus stellar parameters (**a**)) effective temperature, **b)** gravity, **c)** microturbolent velocity) in the three clusters. In each panel, the stars of NGC 4815 are in green, those of Trumpler 20 in magenta, and those of NGC 6705 in blue.

Table 3. σ and Δ for abundance ratios in each cluster.

El	Mean	σ^a	Δ^b
Tr20			
N (number of member stars) = 13			
[Fe/H]	0.17	0.05	0.07
[Si/Fe]	–0.02	0.03	0.08
[Ca/Fe]	–0.05	0.03	0.08
[Mg/Fe]	0.04	0.03	0.09
[Ti/Fe]^c	–0.10	0.04	0.08
[Ni/Fe]	–0.06	0.05	0.08
[Cr/Fe]	–0.08	0.02	0.08
NGC 4815			
N (number of member stars) = 5			
[Fe/H]	0.03	0.05	0.10
[Si/Fe]	–0.02	0.05	0.09
[Ca/Fe]	–0.06	0.03	0.09
[Mg/Fe]	0.14	0.10	0.13
[Ti/Fe]^a	–0.16	0.07	0.08
[Ni/Fe]	–0.09	0.02	0.09
[Cr/Fe]	–0.15	0.03	0.09
NGC 6705			
N (number of member stars) = 21			
[Fe/H]	0.14	0.06	0.14
[Si/Fe]	0.03	0.05	0.16
[Ca/Fe]	–0.02	0.05	0.14
[Mg/Fe]	0.20	0.09	0.17
[Ti/Fe]^a	–0.05	0.07	0.14
[Ni/Fe]	0.01	0.03	0.16
[Cr/Fe]	–0.07	0.05	0.15

Notes. $^{(a)}$ σ is the standard deviation of all elements; $^{(b)}$ Δ is the average uncertainty in the abundances ($\Delta = \langle\delta\rangle$); $^{(c)}$ [Ti/Fe] is computed using only Ti I lines.

that this approach might overestimate the error on [El/Fe], since the error on [El/H] and [Fe/H] are likely correlated. The best approach should be to consider the effect on [El/Fe] due to the errors on the atmospheric parameters, but these kind of errors are not included in the present release. For the error on [Fe/H] we used the values in column σ(Fe I) of Table 2. If we consider the best determined element, such as iron, we note that σ is lower than Δ. This is true for most of the other elements with the possible exception of Mg and Ti which have a larger scatter in NGC 6705 and NGC 4815. Thus, we can conclude that, with the present level of precision, these open clusters are homogeneous with respect to their content in α-elements (Ti, Si, Ca, Mg) and iron-peak elements (Fe, Ni, Cr). In Figs. 3–5 these results are reinforced: the abundance ratios of clusters do not show any correlation with [Fe/H], and within the errors, they are homogeneous.

5.2. Chemical patterns

Having established the chemical homogeneity of these elements in the three clusters under analysis, we can compare their abundance patterns using the average abundances as representative of the entire cluster. In Fig. 6, we graphically present these results. An important feature is the comparison of the average abundance ratios in the three open clusters. As said in the previous sections, Trumpler 20, NGC 4815, and NGC 6705 are located at similar distances from the Galactic centre. They mainly differ in terms of age, cluster mass, and metallicity [Fe/H]. In terms of [Fe/H],

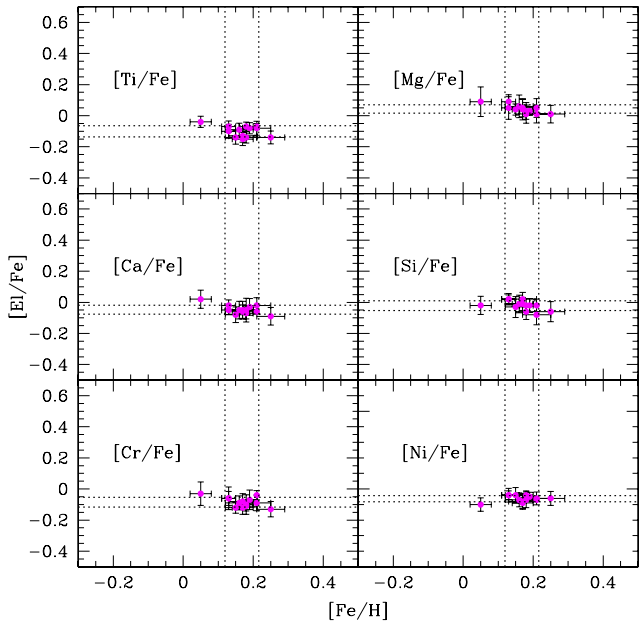

Fig. 3. Abundance ratios versus [Fe/H] for individual member stars in Tr20. Errors on abundance ratios [El/Fe] are computed by summing the errors in [El/H] in quadrature and the errors on [Fe/H]. In each panel, the rectangular region shown by intersection of the four dotted lines indicates the 1σ area around the average value.

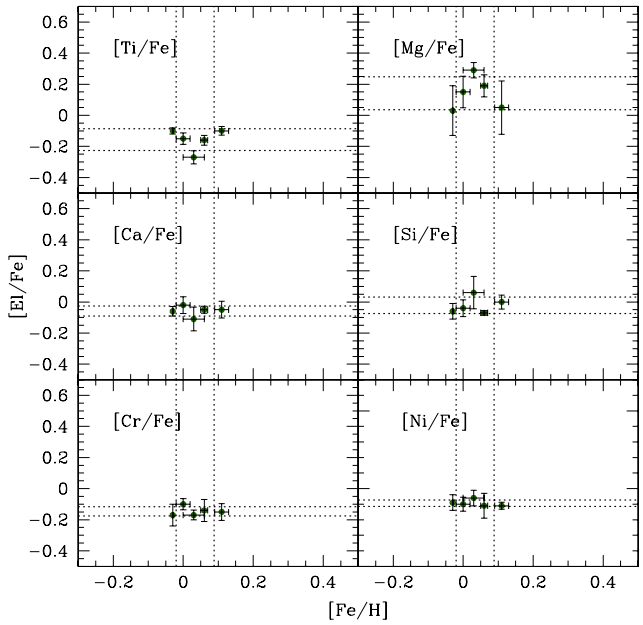

Fig. 4. As in Fig. 3, but for NGC 4815.

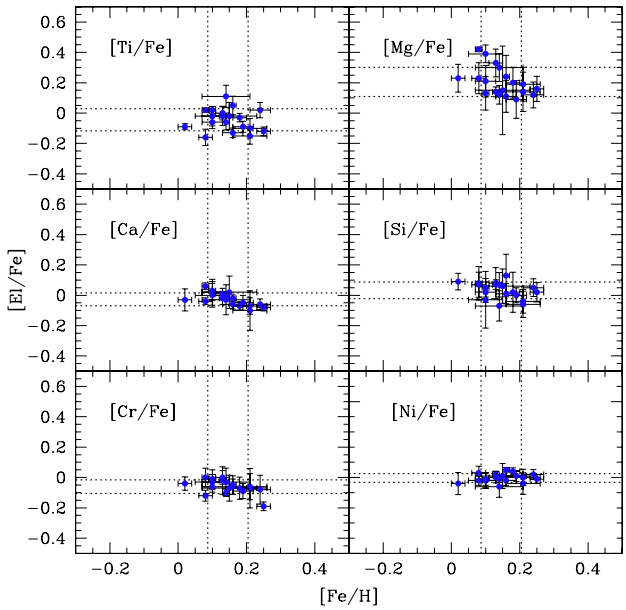

Fig. 5. As in Fig. 3, but for NGC 6705.

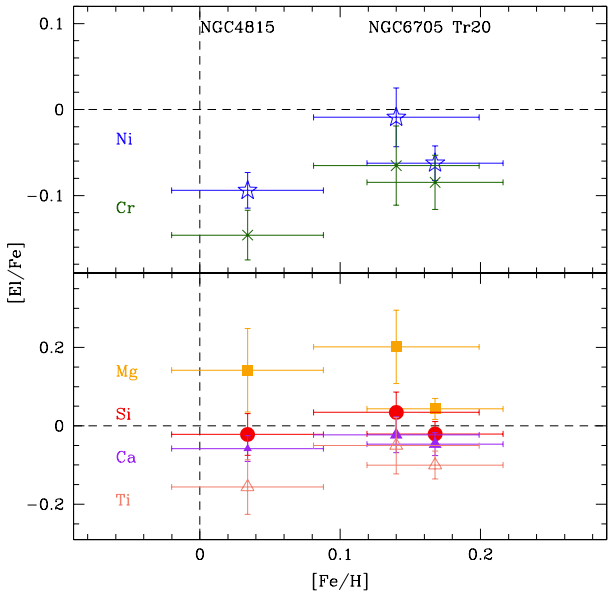

Fig. 6. Average values of the four α-elements (Ca, Si, Ti, and Mg) in the *bottom panel*. Results of iron-peak elements (Ni, Cr) are shown in the *upper panel*. Clusters are ordered by [Fe/H]: NGC 4815 is the first cluster on the left, NGC 6705 in the middle, and Trumpler 20 on the right side. The errors are the standard deviation, σ, computed for member stars of each clusters. The colour and symbol codes are the following: green crosses for [Cr/Fe], blue stars for [Ni/Fe], red circles for [Si/Fe], purple filled triangles for [Ca/Fe], orange squares for [Mg/Fe], and empty salmon pink triangles for [Ti/Fe].

the metal poorest cluster (NGC 4815) and the metal richest one (Trumpler 20) differ $\sim 2\sigma$.

Inspecting Fig. 6, we note that each cluster shows unique features with respect to the other clusters: Trumpler 20 has solar [Si/Fe], [Mg/Fe], and [Ca/Fe] and is slightly depleted in [Ti/Fe], [Ni/Fe] and [Cr/Fe]. The cluster NGC 4815 is solar in [Si/Fe], and [Ca/Fe], and is slightly depleted in [Ti/Fe], [Cr/Fe] and [Ni/Fe], and enhanced in [Mg/Fe]. The cluster NGC 6705 is solar in [Ti/Fe], [Si/Fe], [Ca/Fe] and [Ni/Fe], while it is enhanced in [Mg/Fe] and depleted in [Cr/Fe]. We statistically quantified the level of significance of the cluster-to-cluster abundance differences by estimating, the following quantity for each abundance ratio in each pair of clusters

$$([\mathrm{El/Fe}]_{\mathrm{cluster1}} - [\mathrm{El/Fe}]_{\mathrm{cluster2}}) \Big/ \sqrt{\left(\delta([\mathrm{El/Fe}]_{\mathrm{cluster1}})^2 + \delta([\mathrm{El/Fe}]_{\mathrm{cluster2}})^2\right)}, \quad (1)$$

where the abundance ratios and their errors are those reported in Table 3. All pairs of comparison are of the order of 1σ with the lowest difference for [Si/Fe] in Trumpler 20 and NGC 4815, and the largest difference for [Ni/Fe] in NGC 6705 and NGC 4815

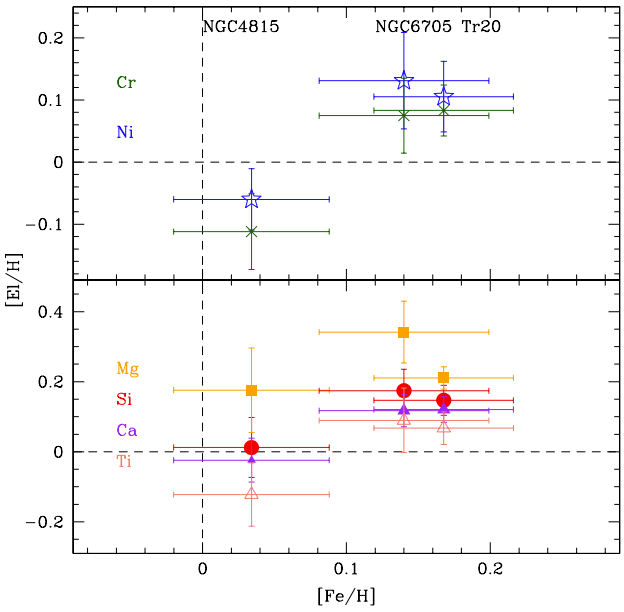

Fig. 7. As in Fig.6, but for [El/H].

differ more than 2σ. In terms of abundance ratios over iron, this suggests that these clusters are statistically very similar, but they differ in their global content of metals. We have thus done the same comparison with the elemental abundances, [El/H]. The results are shown in Fig.7, from which we see how the abundances of NGC 4815 differ from those of Trumpler 20 and NGC 6705 for all elements. We recomputed the level of significance of the cluster-to-cluster abundance differences and find that NGC 4815 differs $\sim 2\sigma$ from the other two clusters in most of its [El/H] abundances.

These differences, especially those of [El/H], can be considered intrinsic characteristics of the chemical composition of the interstellar medium (ISM) from which each cluster was born since the analysis was performed in a fully homogeneous way from the target selection to the observational strategy, data reduction, and abundance analysis. Even if at present Trumpler 20, NGC 4815 and NGC 6705 are located at similar distances from the Galactic centre (GC; although NGC 6705 is on the opposite side of the Sun-Galactic centre line) a tentative first conclusion might be that they did not originate in an ISM with the same composition. In particular the difference in their mean metallicity is relevant with NGC 4815 having a lower metallicity (within 2σ) than the other two clusters. This can be obtained, at least, in three different ways: *i)* the ISM is not azimuthally homogeneous, and areas located at similar radii might have a different chemical composition due to local enrichment and to incomplete mixing; *ii)* the clusters might have moved from their place of birth, and thus, they might reflect the chemical composition at a different radius with respect to their present position; *iii)* due to the different ages of the clusters, their mean metallicity and abundance ratios might be a signature of the temporal chemical evolution of the Galactic disk. A comparison with the field population in the approximation that the migration does not dominate its distribution is useful for checking these hypotheses. In Sect. 6, we describe a comparison with two different Galactic chemical evolution models to search for a possible explanation about the origin of the abundance ratios in these inner-disk open clusters.

5.3. A comparison of abundance distributions in the field and clusters

The uniformity of the analysis of cluster and field stars offers the possibility of seeing differences in abundances at a level not possible before, when heterogeneous samples and analysis methods were considered. We remind us that our comparison is done with stars belonging to different evolutionary stages, such as solar neighbourhood turn-off stars, open cluster clump giants, and inner disk giants. Even though these samples are subjected to a homogeneous analysis, systematic offsets in abundances could arise. Indeed, as a matter of caution when comparing stars in different evolutionary stages, we shall recall a recent analysis of stellar spectra for stars in the open cluster M 67. Önehag et al. (2011) analysed a solar twin in M 67, a dwarf star with stellar parameters very similar to those of the Sun and found an [Fe/H] ratio of +0.02 dex and an [El/Fe] ratio within 0.03 dex of the solar values. This is in contrast to analysis of evolved giant stars in the same cluster for which Yong et al. (2005) found an [Fe/H] ratio that is very close to the solar value but with abundance ratios that differ significantly from the solar values. However, more than the difference in evolutionary stages we consider that different methods and different atomic data might affect the results of the analysis of Önehag et al. (2011) and of Yong et al. (2005). A contrasting example can be found in the study of IC 4615 (Pasquini et al. 2004), who analysed both dwarf and giant stars, for which no differences in the chemical composition were found.

As also pointed by Meléndez et al. (2008), the use of the same set of lines and the choice of a common solar abundance scale for the normalisation of the stellar results are of great importance and are among the main strengths of our analysis. We recall that different conclusions were drawn, for instance, from a comparison of bulge and thick disk stars in Fulbright et al. (2007) and Meléndez et al. (2008). Those differences are probably due to the heterogeneous comparison in the former paper, where their bulge giant results are compared with literature values for main sequence and turn-off disk stars in the solar neighbourhood (Bensby et al. 2005; Reddy et al. 2006) analysed with a different line list and normalised to a different solar zero-point. In the *Gaia*-ESO survey analysis: all stars are analysed as homogeneously as possible, and these systematic effects should be reduced.

In Fig. 8, we show the abundance ratios, [El/Fe] versus [Fe/H], of solar neighbourhood dwarf stars for inner disk/bulge giant stars and of clusters. We note that elemental abundances of stars in open clusters are consistent and within the error with the trends of [El/Fe] versus [Fe/H] for almost all elements in field stars. However, cluster stars show some differences from field stars having the same [Fe/H].

A statistical way to compare two distinct populations is to compare their cumulative distributions. In our case, we want to probe possible differences in the chemical composition of two populations; thus, we compare the cumulative distribution of their elemental abundance ratios. For each cluster, we have selected only field stars for the comparison (both solar neighbourhood and inner-disk/bulge stars) in the same metallicity range, 0.2 dex, that are centred around the mean metallicity of the cluster stars: $0.05 \leq$ [Fe/H] < 0.25 for Trumpler 20, $0.0 \leq$ [Fe/H] < 0.2 for NGC 6705, and $-0.1 \leq$ [Fe/H] < 0.1 for NGC 4815. The cumulative distributions of abundance ratios are shown in Figs. 9–11. When the two distributions are closer, the probability is higher that they come from populations sharing the same chemical composition. For instance, the [Ca/Fe] distribution in Tr 20 and in the solar neighbourhood stars have a

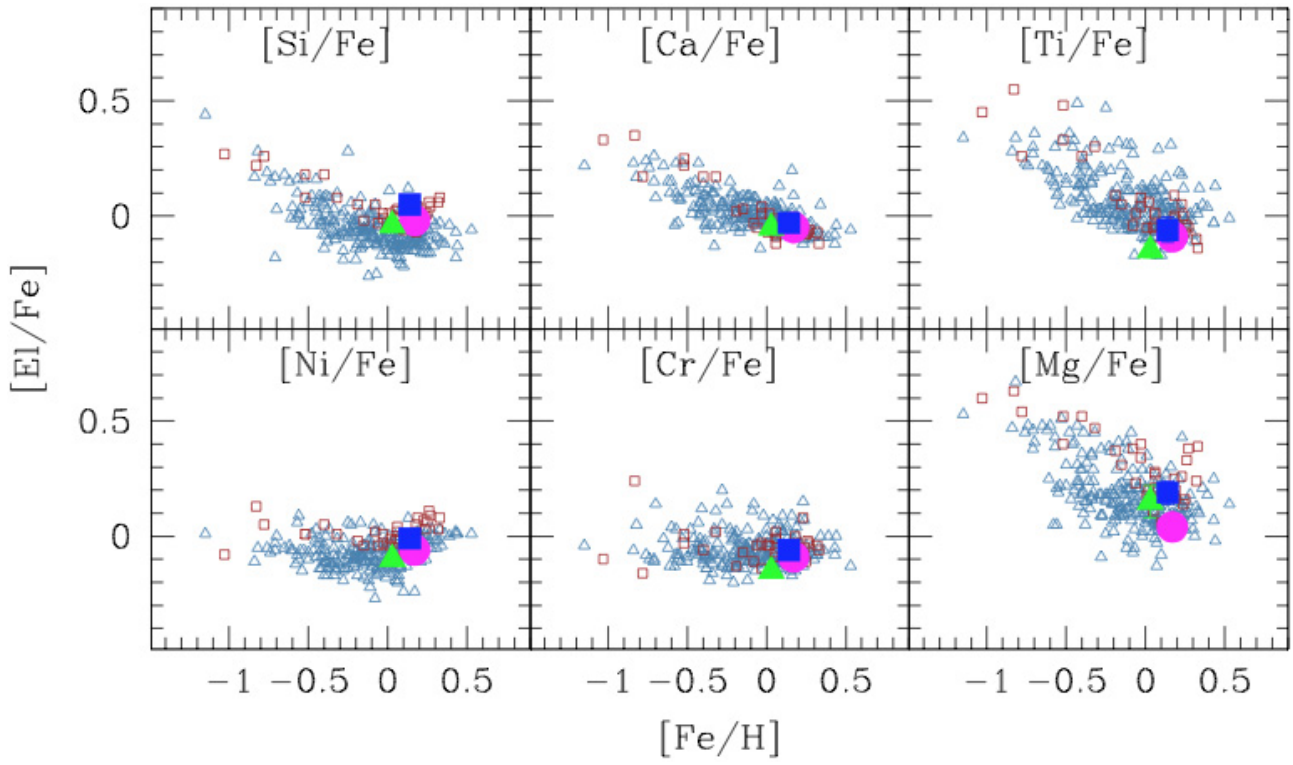

Fig. 8. Abundance ratios in field and open cluster stars: the abundance ratios [El/Fe] versus [Fe/H] of solar neighbourhood dwarf stars (cyan empty triangles), and inner disk/bulge giant stars (red empty squares). Clusters are represented by their average values: Trumpler 20 (magenta filled circle), NGC 4815 (green filled triangle), and NGC 6705 (blue filled square).

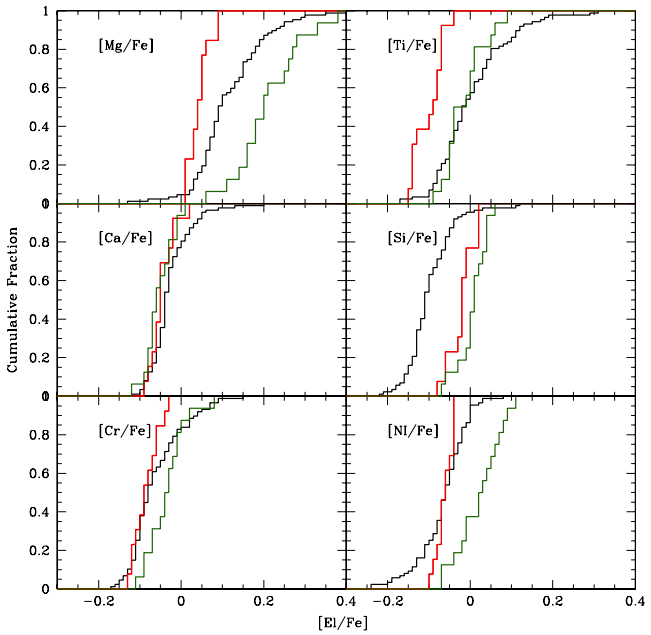

Fig. 9. Comparison of cumulative distribution of the Trumpler 20 abundance ratios (red curves) having the solar neighbourhood turn-off stars with the same metallicity (black curves) and the inner disk/bulge giant stars (green curves).

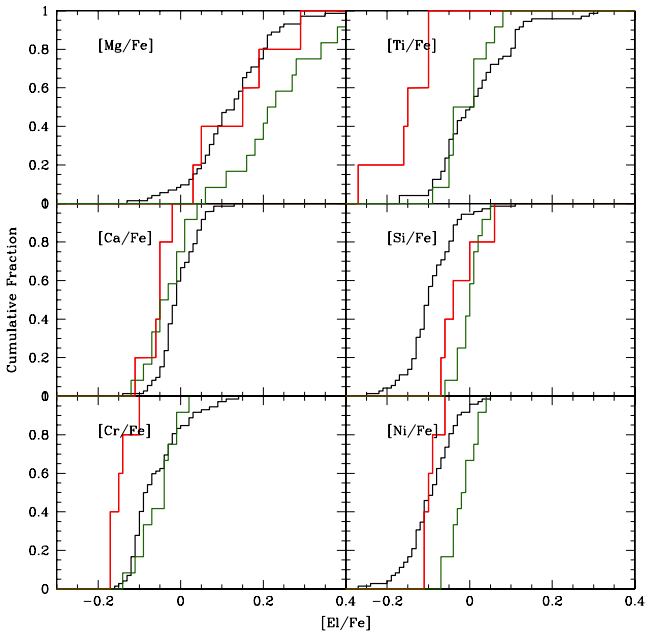

Fig. 10. As in Fig. 9, but for NGC 4815.

probability of ~60% to derive from the same population, while the probability is lower than 1% for [Mg/Fe]. For NGC 4815, the highest probabilities of similar distributions are for [Mg/Fe] (~90%), [Ni/Fe] (~50%), and [Si/Fe] (~20%) in NGC 4815 and in the solar neighbourhood. For NGC 6705, the probabilities that the cluster and inner-disk stars came from similar populations are [Cr/Fe] (~30%), [Ca/Fe] (~50%), [Mg/Fe] (~70%), [Ni/Fe] (~80%), and [Ti/Fe] (~10%). Due to the small number statistics of our analysis we recall that the probabilities associated with the statistical Kolmogorov-Smirnov test have a limited confidence and are only indicative.

In Fig. 9, we have the results for Trumpler 20: this cluster is indistinguishable from the field population in its iron-peak

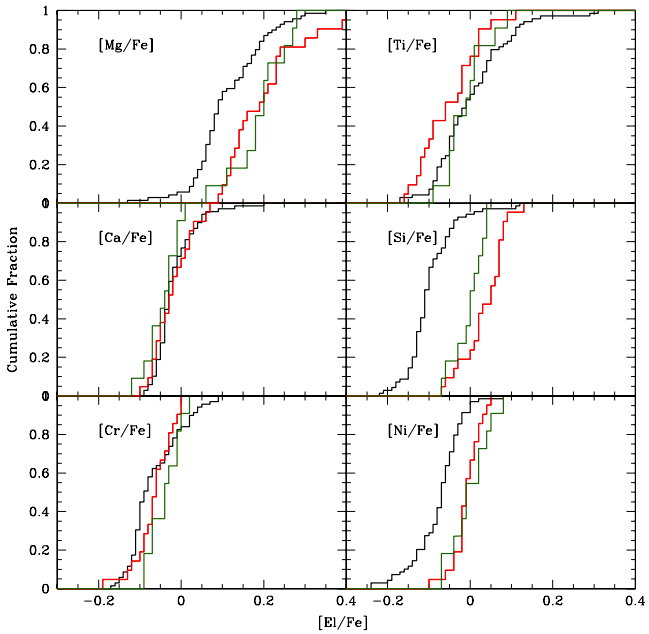

Fig. 11. As in Fig. 9, but for NGC 6705.

elements. The alpha-elements do not all behave in the same way: two of them are remarkably under-abundant compared to field stars with the same metallicity (Mg and Ti), while Ca and Si are distributed similarly to the inner-disk/bulge stars. In Fig. 10 we show the results for NGC 4815, which exhibits a clear under-abundance of Ti, and has [Si/Fe] between the solar neighbourhood and inner disk stars, while Mg and Ca are similar to the solar neighbourhood sample. Among the iron-peak elements, Cr is slightly lower than that in the solar neighbourhood sample, while Ni has the same distribution. In Fig. 11, we present the results for NGC 6705: the behaviour of this cluster is very similar to that of stars located in the inner-disk/bulge, having a similar distribution as Mg, Ti, Ca, Cr, and Ni. Only Si is enhanced with respect to both solar neighbourhood and inner-disk stars.

5.4. Ti abundances in stars of different type

Titanium is evidently more under-abundant in Trumpler 20 and NGC 4815 than in the field population with the same [Fe/H] (see Figs. 9 and 10). Thus it might be a good tracer of the different abundance patterns of these two populations. To prove that this difference is real and not due to NLTE over-ionisation effects in the considered range of stellar parameters, we have plotted [TiII/FeII] – [TiI/FeI] vs. $T_{\rm eff}$, as done by D'Orazi & Randich (2009), and also [TiII/FeII] – [TiI/FeI] vs. log g and ξ (Fig. 12). In their study of the open clusters IC 2602 and IC 2391, D'Orazi & Randich (2009) indeed found some trends of [El/Fe] vs. $T_{\rm eff}$ for various elements. These effects were already found for old field stars by Bodaghee et al. (2003) and by Gilli et al. (2006), who explained them as due to NLTE effects. Other explanations were given from Adibekyan et al. (2012) who analysed a large sample of F-G-K stars for which they studied the relation between [Ti/TiII] and $T_{\rm eff}$. They found a trend that they explained with problems associated with the differential analysis or with an incorrect opacity in the model atmospheres. For Ca and Ti, D'Orazi & Randich (2009) obtained decreasing trends with temperature with cooler stars having lower [Ca/Fe] and [Ti/Fe] than hotter stars in the same cluster. They proposed that the young age of their stars and the enhanced levels of chromospheric activity affect them by NLTE over-ionisation (see their Fig. 4). This trend is completely absent in the three panels of Fig. 12: [TiII/FeII] – [TiI/FeI] is almost consistent with zero along the whole $T_{\rm eff}$, log g and ξ ranges. This is likely due to the older age of our stars and reassures us about the use of titanium as a reliable tracer of the abundance patterns of open clusters. We also did a computation of the NLTE effects on a sample of TiI and TiII lines employed in the analysis of the *Gaia*-ESO Survey. We found that the NLTE correction for TiI are of the order of +0.06 dex on average, while TiII is not affected by NLTE effects (Bergemann, priv. comm.).

6. The origin of the abundance ratios in the inner open clusters

In this section, we discuss what we can learn about the origin of the inner disk open clusters from their abundance patterns. We discuss only elements which are not affected by stellar evolution, and, thus, direct tracers of the ISM composition at the epoch when the cluster formed: the α- and iron-peak elements. We compare their abundance ratios in the field and cluster populations with the predictions of two different chemical evolution models (Magrini et al. 2009; Romano et al. 2010, hereafter M09 and R10, respectively), which are briefly described below.

Model of Romano et al. (2010). The model of R10 is based on the two-infall model case B for the chemical evolution of the Galaxy. A thorough discussion of the adopted formalism and basic equations can be found in Chiappini et al. (1997, 2001). Here, we briefly recall the overall evolutionary scenario. The inner halo and thick disk of the Milky Way are assumed to form on a relatively short timescale (about 1 Gyr) out of a first infall episode, whereas the thin disk forms inside-out (Matteucci & Françoís 1989) on longer timescales (7 Gyr in the solar vicinity) during a second independent episode of extragalactic gas infall. The Galactic disk is approximated by several independent rings, 2 kpc wide. Radial flows and outflows are not considered here. The adopted star-formation rate (SFR) is proportional to both the total mass and the gas surface densities. The efficiency of conversion of gas into stars is higher during the halo/thick-disk phase than during the thin-disk phase. Furthermore, it drops to zero every time the gas density drops below a critical density threshold. The stellar lifetimes are taken into account in detail. As for the stellar IMF, the Kroupa et al. (1993) IMF is assumed in the 0.1−100 $M_{\odot}$ mass range. The rate of SNIa explosions is calculated as in Matteucci & Greggio (1986). The SNeIa explode in close binary systems when a CO white dwarf has reached a critical mass limit because of accretion of hydrogen-rich matter from a main-sequence or red giant companion. The yields for SNeIa are taken from Iwamoto et al. (1999) model W7. As for single stars, several sets of stellar yields are analysed by R10 (see their Table 2). Here we show the results of their model 15, which adopts the yields by Karakas (2010) for low- and intermediate-mass stars (1−6 $M_{\odot}$), the yields of rotating massive stars by the Geneva group (see R10, their Table 1 for references) for helium, carbon, nitrogen and oxygen, and the yields of Kobayashi et al. (2006) for heavier elements produced by Type II supernovae and hypernovae with progenitor masses in the range 13−40 $M_{\odot}$. The available stellar yields are interpolated in the mass range 6−13 $M_{\odot}$ and extrapolated up to 100 $M_{\odot}$ (see R10 for details). The tabulated yields are adopted as published, i.e. without ad hoc adjustments to reproduce the data. Notwithstanding this, model 15 provides a good fit to the abundance ratios of most chemical elements in the Milky Way's stars.

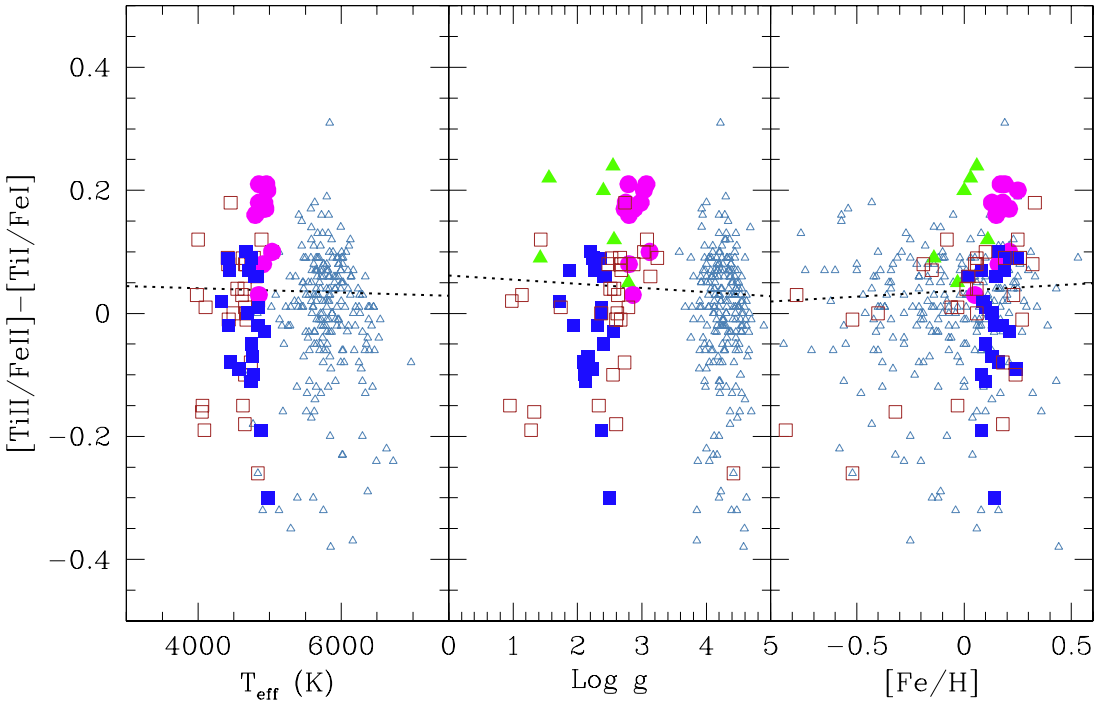

Fig. 12. [TiII/Fe] – [TiI/Fe] vs. $T_{\rm eff}$, log g, and [Fe/H] in the Milky Way field stars and in the cluster member stars. Symbols as in Fig. 8. The dotted lines are the weighted least mean square fits to the data.

Model of Magrini et al. (2009). The model adopted by M09 is a generalisation of the multi-phase model by Ferrini et al. (1992), originally built for the solar neighbourhood, and subsequently extended to the entire Galaxy (Ferrini et al. 1994) and to other disk galaxies (e.g., Mollá et al. 1996; Mollá & Díaz 2005; Magrini et al. 2007). The detailed description of the general model is in the above mentioned papers. The main assumptions of the model are that the Galaxy disk is formed by infall of gas from the halo and from the intergalactic medium. The adopted infall follows an exponentially decreasing law. This produces an inside-out formation scenario, where the inner parts of the disk evolve more rapidly than the outer ones. As in the R10 model, radial flows, stellar migrations, and gas outflows are not considered. The stellar lifetimes are taken into account in detail and the following choices for the stellar yields were made: for low- and intermediate-mass stars ($M < 8\ M_{\odot}$) they use the yields by Gavilán et al. (2005) for both values of the metallicity ($Z = 0.006$ and $Z = 0.02$). For stars in the mass range $8\ M_{\odot} < M < 35\ M_{\odot}$ they adopted the yields by Chieffi & Limongi (2002) for $Z = 0.006$ and $Z = 0.02$. They estimated the yields of stars in the mass range $35\ M_{\odot} < M < 100\ M_{\odot}$, which are not included in the tables of Chieffi & Limongi (2004), by linear extrapolation of the yields in the mass range $8\ M_{\odot} < M < 35\ M_{\odot}$. In the case of Ti, M09 increased the yields by a factor of 2 to reproduce the observations. The rate of SNIa explosions is calculated as in Matteucci & Greggio (1986) and their yields are taken from the model CDD1 by Iwamoto et al. (1999). The IMF by Kroupa et al. (1993) is adopted.

Comparison models vs. data. In Fig. 13, we show the results of the two models: R10 in panel a) and M09 in panel b). The curves refer to different Galactic radii, 4 kpc, 6 kpc, and 8 kpc. Both models are those originally published by R10 and M09 and are not modified to reproduce the *Gaia*-ESO Survey data. Thus, the agreement with the data and the similarity of their predictions for the Solar radius are encouraging, even if there are some discrepant elements. The only exception is Ni for which different yields are adopted by R10 and M09. We note also that the stellar yields adopted in both models are not able to reproduce the trends of [Ti/Fe] vs. [Fe/H], as already noticed in the original papers.

Notwithstanding the agreement at the Solar radius, the two models show a different behaviour in the inner disk, where different assumptions of the infall and SFRs are made. This might be ascribed to the paucity of observational constraints in the inner disk when the two models were designed. We indeed note that the model curves in panel a) reach higher metallicities (by ~0.2 dex) at the innermost radius because of the more intense SFR, but the predicted [El/Fe] ratios are pretty much the same. In panel b), the evolution of the α- and iron-peak elements behaves differently with respect to the Galactocentric radius: while the iron-peak elements are insensitive to the choice of the Galactocentric radius, the α-elements are more enhanced in stars born at $R \sim 4$ kpc than at the Solar radius. This can be easily explained with the short time scales for the gas consumption in the inner part of the disk due to the high SFR, which typically produce high α over iron abundances. On the other hand, the iron-peak elements are insensitive to the radius since they behave to first order, as iron.

For some α-elements, Si, Mg, and marginally Ca and Ti, both the inner-disk/bulge stars and NGC 6705 are in better agreement with the curves corresponding to the innermost radii of M09, which are between 4 and 6 kpc from the Galactic centre. On the other hand, the α abundance ratios of Trumpler 20 and of NGC 4815 agree better with the curve corresponding to their present radius in M09 and with the curves of R10. For the iron-peak elements, the behaviour of the three clusters is very similar and in agreement with the model curves, of both M09 and R10, which do not predict strong variation in these ratios with the Galactocentric radii.

The comparison of the abundance ratios to the model curves together with the similarity observed between the cumulative

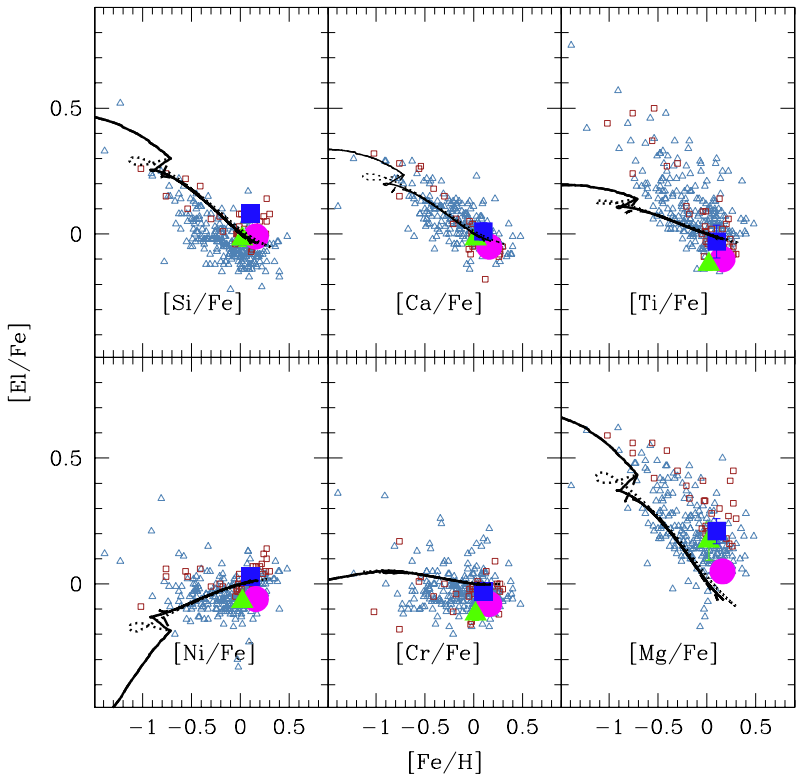

(a) R10

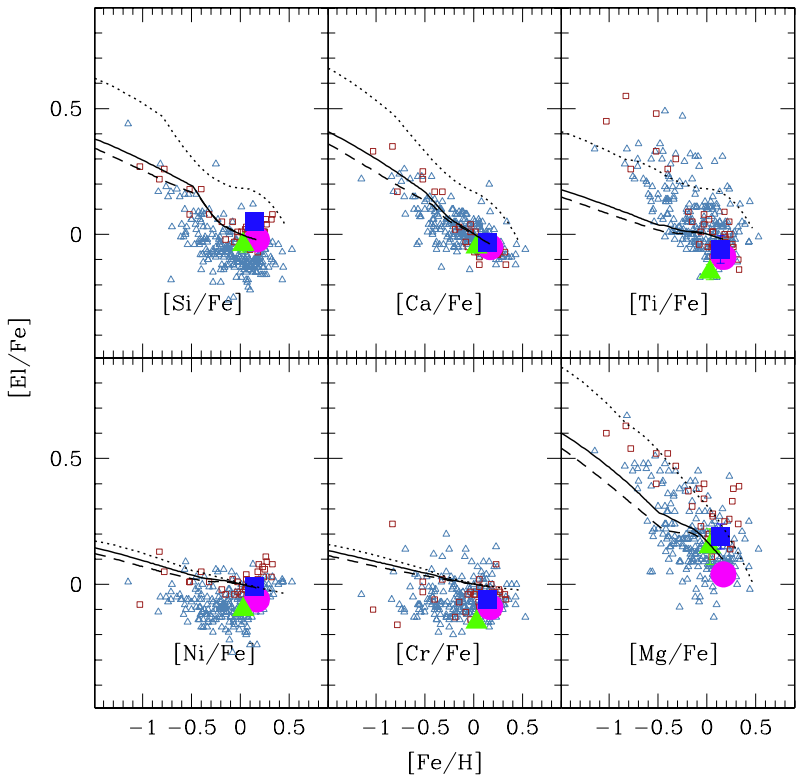

(b) M09

Fig. 13. Abundance ratios in field and open cluster stars: abundance ratios [El/Fe] versus [Fe/H] of solar neighbourhood dwarf stars (cyan empty triangles), of inner disk/bulge giant stars (red empty squares), of stars in Trumpler 20 (magenta filled circle), in NGC 4815 (green filled triangle), and NGC 6705 (blue filled square). In panel **a)** the curves are the model of R10 at three R_{GC}: 4 kpc (dotted line), 6 kpc (continuous line), and 8 kpc (dashed line). The curves shown in panel **b)** are obtained with the model of M09. The theoretical ratios are normalised to the solar abundances predicted by each model, with the exception of [Mg/Fe] in M09 model, which is displaced by other +0.15 dex to match the data.

distributions of abundance ratios and of the solar neighbourhood and inner-disk/bulge stars gives us a "chemical" indication of the birthplace of the three inner-disk clusters under analysis: the good agreement of the [α/Fe] abundance ratio of Trumpler 20 and NGC 4815 with the curves at ∼6−8 kpc for both models and with the abundance ratios of solar neighbourhood stars is a reasonable indication that they were not born very far from their present location. On the other hand, the good agreement within the error of some abundance ratios of NGC 6705 with M09 curves for radii ∼4−6 kpc and with the observations of inner-disk/bulge stars (see Fig. 11) might indicate that it has moved towards its present position from an inner birthplace. This agrees with the orbit determination done for this cluster in Magrini et al. (2010) with a perigalacticon of ∼5 kpc and apogalacticon of ∼9 kpc. Under this scenario, a revision of the basic assumptions of the model of R10 are required for the model to be able to predict higher SFRs/steeper abundance gradients in the inner disk and to face the *Gaia*-ESO Survey abundance data for those clusters. For instance, the inclusion of a bar in the model could lead to enhanced star formation in the inner Galactic region (see, e.g., Wang et al. 2012). In addition, the effect of local inhomogeneities, radial flows, stellar migration, and outflow should not be neglected in next generation of chemical evolution models.

7. Summary

In this paper, we present the analysis of abundance ratios in open clusters and field stars obtained in the first six months of the *Gaia*-ESO Survey. We studied three old/intermediate-age open clusters: NGC 6705, NGC 4815, and Trumpler 20. For the three clusters, we find that: *i)* the clusters are internally homogeneous in the considered elements (four α-elements, Si, Ca, Mg, Ti, and three iron-peak elements, Fe, Ni, Cr); *ii)* the three clusters have similar [El/Fe] abundance patterns, but a different global metallicity and, consequently, different [El/H] patterns; *iii)* a comparison of the cumulative distributions of abundance ratios shows that the abundance ratios of NGC 6705 are very similar to those of inner-disk/bulge stars studied by the *Gaia*-ESO Survey, while the abundance patterns of NGC 4815 and Trumpler 20 do not perfectly match either the solar neighbourhood stars or the inner-disk/bulge stars. We finally compare the field and cluster abundance ratios to two chemical evolution models (M09 and R10) and find generally a good agreement for the solar neighbourhood. The predictions of the models differ for the inner disk. The α-enhancement of NGC 6705 places it in better agreement with the model curves of M09 for Galactocentric radii from 4 to 6 kpc, and supports an inner birthplace for it with the better agreement for the distributions of abundance ratios in the inner-disk/bulge sample.

In conclusion, the first results from the *Gaia*-ESO Survey show their huge potential by giving new constraints to our view of the Galactic chemical evolution, exploring areas of our Galaxy that have yet to be studied, and, moreover, putting many stellar populations on exactly the same scale for the first time.

Note added in proof. During the final editing phases of the present manuscript, a paper on the chemical composition of Trumpler 20 appeared on astro-ph (Carraro et al. 2014). The two works were carried out independently, despite having a co-author in common and both works come to similar conclusions on the average metallicity of Trumpler 20 with $[Fe/H] = 0.09 \pm 0.10$ dex (with $12 + (Fe/H)_\odot = 7.50$) – i.e., 0.14 dex in our scale – in Carraro et al. (2014).

Acknowledgements. We thank the Referee for her/his comments and suggestions which improved our manuscript. We acknowledge support from INAF and Ministero dell'Istruzione, dell'Universitá e della Ricerca (MIUR) in the form of grant "Premiale VLT 2012". The results presented here benefited from discussions in three *Gaia*-ESO workshops supported by the ESF (European Science Foundation) through the GREAT (*Gaia* Research for European Astronomy Training) Research Network Program (Science meetings 3855, 4127 and 4415). This work was partially supported by the *Gaia* Research for European Astronomy Training (GREAT-ITN) Marie Curie network, funded through the European Union Seventh Framework Programme [FP7/2007-2013] under grant agreement No. 264895. T.B. was funded by grant No. 621-2009-3911 from The Swedish Research Council. This work was partly supported by the European Union FP7 programme through ERC grant number 320360. This work was partly supported by the Leverhulme Trust through grant RPG-2012-541. I.S.R. gratefully acknowledges the support provided by the Gemini-CONICYT project 32110029. This research has made use of the SIMBAD database, operated at the CDS, Strasbourg, France.

References

Adibekyan, V. Z., Sousa, S. G., Santos, N. C., et al. 2012, A&A, 545, A32
Allende Prieto, C., Majewski, S. R., Schiavon, R., et al. 2008, Astron. Nachr., 329, 1018
Andreuzzi, G., Bragaglia, A., Tosi, M., & Marconi, G. 2011, MNRAS, 412, 1265
Andrievsky, S. M., Spite, M., Korotin, S. A., et al. 2007, A&A, 464, 1081
Baglin, A., Auvergne, M., Boisnard, L., et al. 2006, 36th COSPAR Scientific Assembly, 36, 3749
Bensby, T., Feltzing, S., Lundström, I., & Ilyin, I. 2005, A&A, 433, 185
Bodaghee, A., Santos, N. C., Israelian, G., & Mayor, M. 2003, A&A, 404, 715
Bonatto, C., Kerber, L. O., Bica, E., & Santiago, B. X. 2006, A&A, 446, 121
Bragaglia, A., & Tosi, M. 2006, AJ, 131, 1544
Carraro, G., Ng, Y. K., & Portinari, L. 1998, MNRAS, 296, 1045
Carraro, G., Villanova, S., & Monaco, L. 2014, A&A, 562, A39
Chen, L., Hou, J. L., & Wang, J. J. 2003, AJ, 125, 1397
Chiappini, C., Matteucci, F., & Gratton, R. 1997, ApJ, 477, 765
Chiappini, C., Matteucci, F., & Romano, D. 2001, ApJ, 554, 1044
Chieffi, A., & Limongi, M. 2002, ApJ, 577, 281
D'Orazi, V., & Randich, S. 2009, A&A, 501, 553
de Laverny, P., Recio-Blanco, A., Worley, C. C., & Plez, B. 2012, A&A, 544, A126
De Silva, G. M., Freeman, K. C., Asplund, M., et al. 2007, AJ, 133, 1161
Dekker, H., D'Odorico, S., Kaufer, A., Delabre, B., & Kotzlowski, H. 2000, Proc. SPIE, 4008, 534
Donati, P., Cantat Gaudin, T., Bragaglia, A., et al. 2014, A&A, 561, A94
Ferrini, F., Matteucci, F., Pardi, C., & Penco, U. 1992, ApJ, 387, 138
Ferrini, F., Molla, M., Pardi, M. C., & Diaz, A. I. 1994, ApJ, 427, 745
Freeman, K. C. 1970, ApJ, 160, 811
Friel, E. D. 1995, ARA&A, 33, 381
Frinchaboy, P. M., Thompson, B., Jackson, K. M., et al. 2013, ApJ, 777, L1
Fulbright, J. P., McWilliam, A., & Rich, R. M. 2007, ApJ, 661, 1152
Gavilán, M., Buell, J. F., & Mollá, M. 2005, A&A, 432, 861
Gieles, M., Portegies Zwart, S. F., Baumgardt, H., et al. 2006, MNRAS, 371, 793
Gilli, G., Israelian, G., Ecuvillon, A., Santos, N. C., & Mayor, M. 2006, A&A, 449, 723
Gilmore, G., Randich, S., Asplund, M., et al. 2012, The Messenger, 147, 25
Grevesse, N., Asplund, M., & Sauval, A. J. 2007, Space Sci. Rev., 130, 105
Gustafsson, B., Edvardsson, B., Eriksson, K., et al. 2008, A&A, 486, 951
Jacobson, H. R., Pilachowski, C. A., & Friel, E. D. 2011, AJ, 142, 59
Janes, K. A. 1979, ApJS, 39, 135
Janes, K. A., & Phelps, R. L. 1994, AJ, 108, 1773
Jofre, P., Heiter, U., Blanco-Cuaresma, S., & Soubiran, C. 2013a [arXiv:1312.2943]
Jofre, P., Heiter, U., Soubiran, C., et al. 2013b, A&A, submitted DOI: 10.1051/0004-6361/201322440
Karakas, A. I. 2010, MNRAS, 403, 1413
Kobayashi, C., Umeda, H., Nomoto, K., Tominaga, N., & Ohkubo, T. 2006, ApJ, 653, 1145
Kroupa, P., Tout, C. A., & Gilmore, G. 1993, MNRAS, 262, 545
Iwamoto, K., Brachwitz, F., Nomoto, K., et al. 1999, ApJS, 125, 439
Lada, C. J., & Lada, E. A. 2003, ARA&A, 41, 57
Magrini, L., Corbelli, E., & Galli, D. 2007, A&A, 470, 843
Magrini, L., Sestito, P., Randich, S., & Galli, D. 2009, A&A, 494, 95
Magrini, L., Randich, S., Zoccali, M., et al. 2010, A&A, 523, A11
Matteucci, F., & Francois, P. 1989, MNRAS, 239, 885
Matteucci, F., & Greggio, L. 1986, A&A, 154, 279

McMahon, R. 2012, Proc. Science from the Next Generation Imaging and Spectroscopic Surveys, ESO Garching, 37 available at http://www.eso.org/sci/meetings/2012/surveys2012
Meléndez, J., Asplund, M., Alves-Brito, A., et al. 2008, A&A, 484, L21
Mermilliod, J.-C. 1996, The Origins, Evolution, and Destinies of Binary Stars in Clusters, ASP Conf. Ser., 90, 475
Mermilliod, J.-C., Mayor, M., & Udry, S. 2009, A&A, 498, 949
Mollá, M., & Díaz, A. I. 2005, MNRAS, 358, 521
Mollá, M., Ferrini, F., & Diaz, A. I. 1996, ApJ, 466, 668
Nordström, B., Mayor, M., Andersen, J., et al. 2004, A&A, 418, 989
Önehag, A., Korn, A., Gustafsson, B., Stempels, E., & Vandenberg, D. A. 2011, A&A, 528, A85
Panagia, N., & Tosi, M. 1981, A&A, 96, 306
Pancino, E., Carrera, R., Rossetti, E., & Gallart, C. 2010, A&A, 511, A56
Pasquini, L., Avila, G., Blecha, A., et al. 2002, The Messenger, 110, 1
Pasquini, L., Randich, S., Zoccali, M., et al. 2004, A&A, 424, 951
Phelps, R. L., Janes, K. A., & Montgomery, K. A. 1994, AJ, 107, 1079
Randich, S., & Gilmore, G. 2012, Proc. Science from the Next Generation Imaging and Spectroscopic Surveys, ESO Garching, 21 available at http://www.eso.org/sci/meetings/2012/surveys2012
Reddy, B. E., Lambert, D. L., & Allende Prieto, C. 2006, MNRAS, 367, 1329
Twarog, B. A., Ashman, K. M., & Anthony-Twarog, B. J. 1997, AJ, 114, 2556
Robin, A. C., Reylé, C., Derrière, S., & Picaud, S. 2003, A&A, 409, 523
Rocha-Pinto, H. J., Flynn, C., Scalo, J., et al. 2004, A&A, 423, 517
Romano, D., Karakas, A. I., Tosi, M., & Matteucci, F. 2010, A&A, 522, A32
Santos, J. F. C., Jr., Bonatto, C., & Bica, E. 2005, A&A, 442, 201
Scott, J. E., Friel, E. D., & Janes, K. A. 1995, AJ, 109, 1706
Sestito, P., Bragaglia, A., Randich, S., et al. 2006, A&A, 458, 121
Sestito, P., Randich, S., & Bragaglia, A. 2007, A&A, 465, 185
Sestito, P., Bragaglia, A., Randich, S., et al. 2008, A&A, 488, 943
Skrutskie, M. F., Cutri, R. M., Stiening, R., et al. 2006, AJ, 131, 1163
van der Kruit, P. C. 2002, The Dynamics, Structure & History of Galaxies: A Workshop in Honour of Professor Ken Freeman, eds. G. S. Da Costa, & H. Jerjen, ASP Conf. Ser., 273, 7
Wang, J., Kauffmann, G., Overzier, R., et al. 2012, MNRAS, 423, 3486
Wu, Z.-Y., Zhou, X., Ma, J., & Du, C.-H. 2009, MNRAS, 399, 2146
Yong, D., Carney, B. W., & Teixera de Almeida, M. L. 2005, AJ, 130, 597
Yong, D., Carney, B. W., & Friel, E. D. 2012, AJ, 144, 95

[1] INAF-Osservatorio Astrofisico di Arcetri, Largo E. Fermi 5, 50125 Firenze, Italy
e-mail: laura@arcetri.astro.it
[2] INAF-Osservatorio Astronomico di Bologna, via Ranzani 1, 40127 Bologna, Italy
[3] Department of Astronomy, Indiana University, Bloomington, USA
[4] Department for Astrophysics, Nicolaus Copernicus Astronomical Center, ul. Rabiańska 8, 87-100 Toruń, Poland
[5] European Southern Observatory, Karl-Schwarzschild-Str. 2, 85748 Garching bei München, Germany
[6] MIT Kavli Institute, Boston, USA
[7] Osservatorio Astronomico di Padova, Vicolo dell'Osservatorio 5, 35122 Padova, Italy
[8] Dipartimento di Fisica, sezione di Astronomia, Largo E. Fermi 2, 50125 Firenze, Italy
[9] Dipartimento di Fisica e Astronomia, via Ranzani 1, 40127 Bologna, Italy
[10] Dipartimento di Fisica e Astronomia, Vicolo dell'Osservatorio 3, 35122 Padova, Italy
[11] Institute of Astronomy, University of Cambridge, Madingley Road, Cambridge CB3 0HA, UK
[12] Osservatorio Astronomico di Palermo, Piazza del Parlamento 1, 90134 Palermo, Italy
[13] Institute of Theoretical Physics and Astronomy, Vilnius University, A. Gostauto 12, 01108 Vilnius, Lithuania
[14] Univ. Bordeaux, LAB, UMR 5804, 33270 Floirac, France
[15] CNRS, LAB, UMR 5804, 33270 Floirac, France
[16] Centro de Astrobiología (INTA-CSIC) PO Box 78, 28691 Villanueva de la Canada, Madrid, Spain
[17] Departamento de Astronomía, Universidad de Concepción, Casilla 160-C, Concepción, Chile
[18] Astronomy Department, University of Geneva, Ch. des Maillettes 51, 1290 Versoix, Switzerland
[19] Research School of Astronomy and Astrophysics, Australian National University, ACT 2611 Canberra, Australia
[20] Lund Observatory, Department of Astronomy and Theoretical Physics, Box 43, 221 00 Lund, Sweden
[21] Astrophysics Group, Keele University, Keele ST5 5BG, UK
[22] Moscow M.V. Lomonosov State University, Sternberg Astronomical Institute, Universitetskij pr., 13, 119992 Moscow, Russia
[23] ASI Science Data Center, 00044 Frascati, Italy
[24] Laboratoire Lagrange (UMR7293), Université de Nice Sophia Antipolis, CNRS, Observatoire de la Côte d'Azur, BP 4229, 06304 Nice Cedex 4, France
[25] Instituto de Astrofísica de Andalucía (IAA-CSIC), Glorieta de la Astronomía, 18008 Granada, Spain
[26] Department of Physics and Astronomy, Uppsala University, Box 516, 75120 Uppsala, Sweden